Chapter 8

Synthesis Characterization of Nanostructured $ZnCo_2O_4$ with High Sensitivity to CO Gas

Juan Pablo Morán-Lázaro, Florentino López-Urías,
Emilio Muñoz-Sandoval, Oscar Blanco-Alonso,
Marciano Sanchez-Tizapa,
Alejandra Carreon-Alvarez, Héctor Guillén-Bonilla,
María de la Luz Olvera-Amador,
Alex Guillén-Bonilla and
Verónica María Rodríguez-Betancourtt

Additional information is available at the end of the chapter

http://dx.doi.org/10.5772/68043

Abstract

In this work, nanostructured $ZnCo_2O_4$ was synthesized via a microwave-assisted colloidal method, and its application as gas sensor for the detection of CO was studied. Typical diffraction peaks corresponding to the cubic $ZnCo_2O_4$ spinel structure were identified at calcination temperature of 500°C by X-ray powder diffraction. A high degree of porosity in the surface of the nanostructured powder of $ZnCo_2O_4$ was observed by scanning electron microscopy and transmission electron microscopy, faceted nanoparticles with a pockmarked structure were clearly identified. The estimated average particle size was approximately 75 nm. The formation of $ZnCo_2O_4$ material was also confirmed by Raman characterization. Pellets fabricated with nanostructured powder of $ZnCo_2O_4$ were tested as sensors using CO gas at different concentrations and temperatures. A high sensitivity value of 305–300 ppm of CO was measured at 300°C, indicating that nanostructured $ZnCo_2O_4$ had a high performance in the detection of CO.

Keywords: spinel, nanoparticles, cobaltite, sensors, characterization, synthesis

1. Introduction

Gas sensors technology has numerous applications in the automotive, industrial, domestic, and security sectors. In the automotive and industrial sectors, gas sensors are necessary to detect toxic and harmful gases for environment protection and human health (i.e., carbon monoxide). Sensor materials based on semiconducting metal oxides are one of the several technologies being used in the detection of pollutants [1]. This type of oxide materials is suitable for gas sensor applications due to their interesting structural, functional, physical, and chemical properties. To date, reports indicate that n-type semiconductor materials, such as SnO_2 [2, 3], ZnO [4], and TiO_2 [5] are most studied in gas sensing area. By contrast, a limited amount research works on p-type oxide semiconductor gas sensors have been found, the most studied being CuO, Co_3O_4, and NiO [6]. However, some sensor parameters such as gas sensitivity and working temperature still need to be improved. Therefore, additional studies are needed to improve the gas sensing characteristics of p-type semiconducting oxides by modifying factors such as synthesis conditions, structure, morphology, and composition.

Among the p-type semiconductors, zinc cobaltite ($ZnCo_2O_4$) is a material with spinel-type structure, which has been mainly used as electrode for Li-ion batteries [7–11] and supercapacitors [12–15], due to its higher electrochemical performances and higher conductivities. To date, sensor devices based on nanostructured spinel $ZnCo_2O_4$ have particularly exhibited an excellent sensitivity toward liquefied petroleum gas [16–18], ethanol [19, 20], acetone [21], Cl_2 [22], formaldehyde [23], and Xylene [24]. Additionally, several references [18–21, 25] reported its poor sensitivity to carbon monoxide (CO). On the other hand, a variety of synthesis methods have been developed on the preparation of $ZnCo_2O_4$ such as combustion [7], thermal decomposition [17], co-precipitation/digestion [18], W/O microemulsion [22], hydrothermal [9, 14], sol-gel [26], and surfactant-mediated method [27]. Recently, the colloidal route assisted by microwave radiation has provided an efficient and low cost synthesis method to obtain different types of nanostructured materials [28–31]. In this simple synthetic process, the addition of a surfactant agent plays a key role in the material's microstructure because the surfactant's ligands adsorb on the particles' surface inhibiting the particle growth and modifying the particles' microstructure [31–34]. Also, microwave radiation provides a rapid evaporation of the precursor solvent and a short reaction time in comparison with conventional heating [35, 36]. With this in mind, the synthesis of nanostructured $ZnCo_2O_4$ was done via a microwave-assisted colloidal method using zinc nitrate, cobalt nitrate, dodecylamine (as surfactant), and ethanol. Consequently, nanostructured $ZnCo_2O_4$ powder was characterized by X-ray powder diffraction (XRD), scanning electron microscopy (SEM), transmission electron microscopy (TEM), and Raman spectroscopy. The potential application of nanostructured $ZnCo_2O_4$ as gas sensor was studied by measuring its sensitivity toward different CO concentrations and working temperatures.

2. Synthesis, characterization, and gas sensing application of $ZnCo_2O_4$

2.1. Synthesis

For the preparation of nanostructured $ZnCo_2O_4$ by microwave-assisted colloidal method, first, 0.947 g of $Zn(NO_3)_2 \cdot xH_2O$ (Zinc nitrate hydrate), 2.91 g of $Co(NO_3)_2 \cdot 6H_2O$ (cobalt nitrate

http://dx.doi.org/10.5772/68043

hexahydrate), and 1 g of $C_{12}H_{27}N$ (dodecylamine) were dissolved separately in 5 mL of ethanol and kept under stirring for 20 min, at room temperature. Then, the cobalt nitrate solution was added drop wise to the dodecylamine solution under stirring. Then, the zinc nitrate solution was slowly added, producing a wine color solution with pH = 2. This resulting colloidal solution was stirred for approximately 24 h. Then, the solvent evaporation was made by a domestic microwave oven (General Electric JES769WK) operated at low power (~140 W). During the evaporation process, microwave radiation was applied for a period of 1 min, over a period of 3 h. The resulting solid material was dried in air at 200°C for 8 h using a muffle-type furnace (Novatech). Finally, the obtained powders were calcined at 500°C for 5 h. For each thermal treatment, a heating rate of 100°C/h was used. The resulting powders were black. The general synthesis process is illustrated in **Figure 1**.

2.2. Experimental techniques

The structural characterization was performed by XRD using a PANalytical Empyrean system (CuKα, λ = 1.546 Å). The XRD patterns were recorded, at room temperature, in the 2θ range of 10–70° using a step size of 0.02°. The morphological characterization was made by SEM, TEM, high-resolution transmission electron microscopy (HRTEM), energy-dispersive X-ray (EDS), and high-angle annular dark-field/scanning transmission electron microscopy (HAADF-STEM). For SEM studies, a FEI-Helios Nanolab 600 system operated at 20 kV was used, while a FEI Tecnai-F30 system operated at 300 kV was used for TEM, HRTEM, EDS, and HAADF-STEM analysis. The optical characterization was done by Raman spectroscopy using a Thermo Scientific DXR confocal Raman with a 633 nm excitation source. The Raman spectrum was recorded from 150 to 800 cm^{-1}, at room temperature, using a Laser power of 5 mW. The gas response (sensitivity) was acquired on pellets of $ZnCo_2O_4$ in the presence of several concentrations (1, 5, 50, 100, 200, and 300 ppm) of CO. The sensor devices were fabricated with 0.350 g of the nanostructured powder of $ZnCo_2O_4$, forming pellets with a thickness of 0.5 mm and a diameter of 12 mm. A TM20 Leybold detector was used to control the gas concentration and the partial pressure, and a digital-multimeter (Keithley) was put into use for the measurement of the electric resistance. A general schematic diagram of the gas sensing measurement system is shown in Ref. [33]. The sensitivity was defined as $S = R_a/R_g$, where R_a is the resistance measured in air and R_g is the resistances in gas [21, 24].

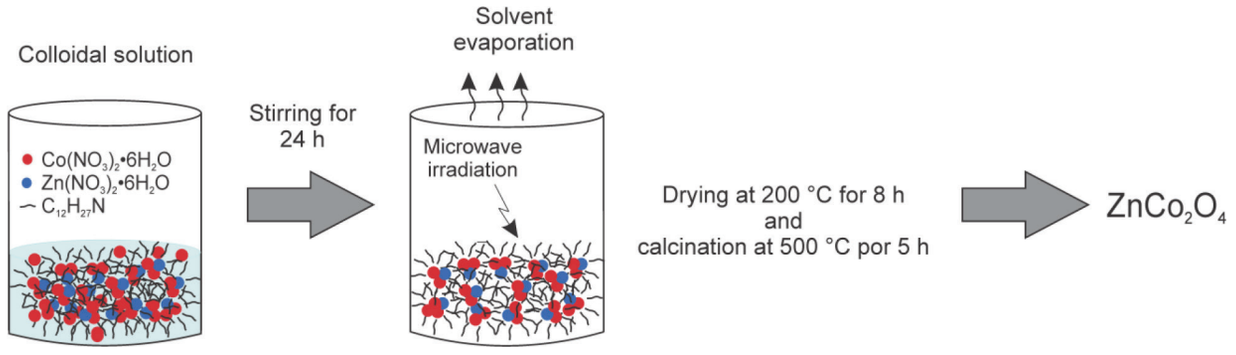

Figure 1. Schematic illustration of the synthesis of $ZnCo_2O_4$.

2.3. Structural analysis

Figure 2 shows a typical XRD pattern of the $ZnCo_2O_4$ powder obtained at a calcination temperature of 500°C. In this pattern, the main phase detected was the $ZnCo_2O_4$ crystal structure, which was identified by the JCPDF #23-1390 file. The sharp and strong peaks indicated a good crystallinity of the $ZnCo_2O_4$ sample. The diffraction peaks corresponded well to the (111), (220), (311), (222), (400), (422), (511), and (440) planes of the $ZnCo_2O_4$ spinel phase situated at 2θ = 18.95°, 31.21°, 36.80°, 38.48°, 44.73°, 55.57°, 59.28°, and 65.14°, respectively. The average crystal size, which was calculated by Scherrer's formula [38], using the XRD (311) plane, was ~24.7 nm. Since no secondary phase was detected in the XRD pattern of the $ZnCo_2O_4$, the synthesis procedure developed in this work allowed to obtain the crystalline phase of $ZnCo_2O_4$ without additional diffraction peaks. Thus, this method of synthesis might also be useful for the preparation of other oxide materials.

2.4. Morphological investigations

Figure 3 shows the surface morphology of the $ZnCo_2O_4$ powder calcined at 500°C with different magnifications. **Figure 3a** exhibits a SEM image at low magnification, which revealed a surface with a high degree of porosity with pores of irregular shape. The average pore size was calculated around 724 nm. This extensive porosity has been associated with the emission of gas during the removal of organic matter in the calcination process [28]. At high magnification (**Figure 3b**), a large number of nanoparticles with irregular shape and size in the range of 50–110 nm were clearly observed. In colloidal chemistry, it is known

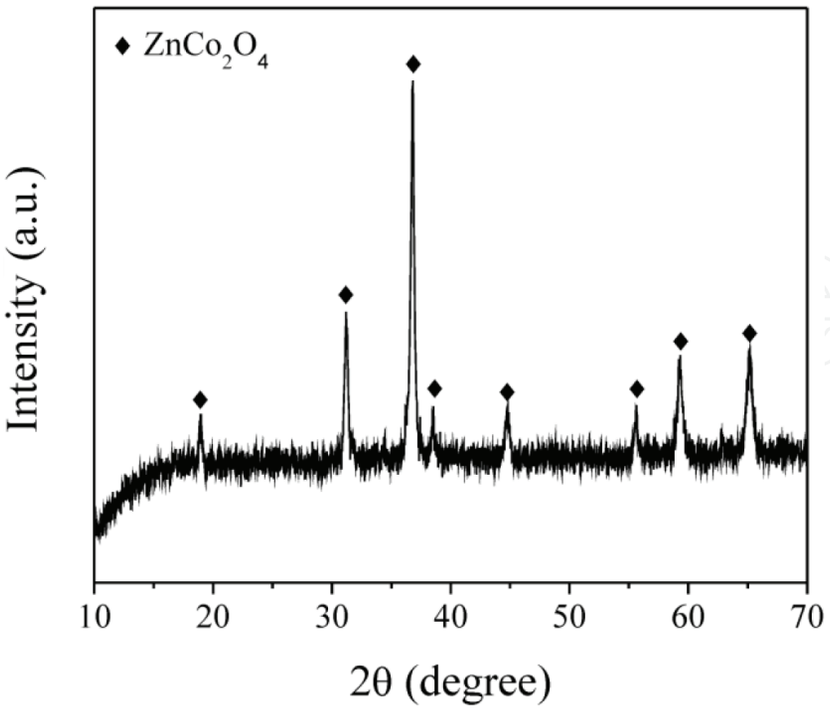

Figure 2. XRD pattern of the $ZnCo_2O_4$ powder after a thermal treatment at 500°C in air [37].

http://dx.doi.org/10.5772/68043

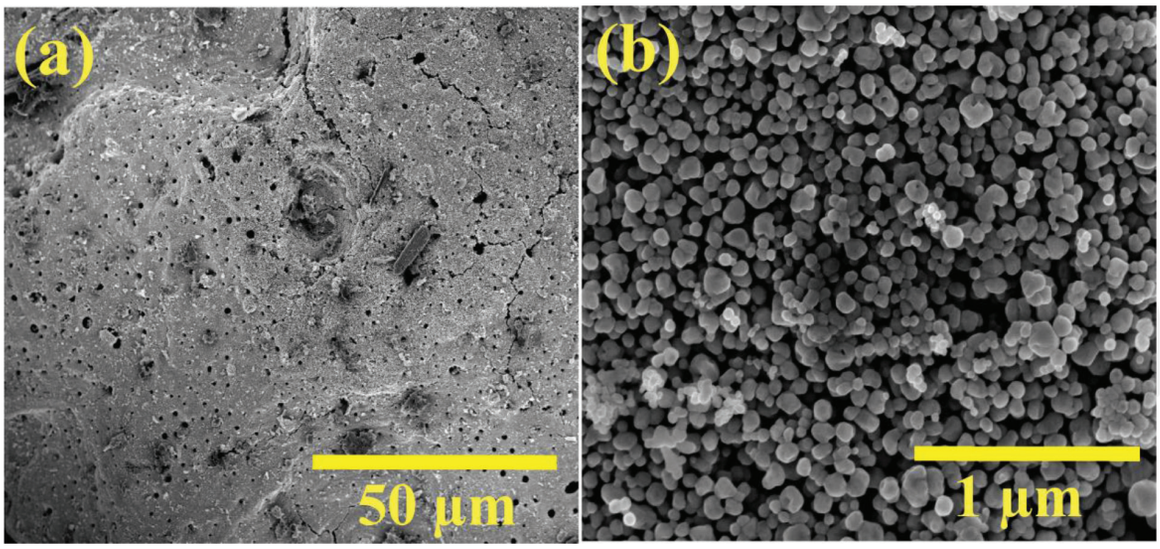

Figure 3. SEM images of the $ZnCo_2O_4$ powder at: (a) low (1,100x) and (b) high magnification (50,000x) [37].

that the formation of nanoparticles follows a nucleation and a growth mechanism [39]. In this mechanism, first, the nucleation is produced when the concentration of reagents reach the supersaturation limit for a short period of time. Consequently, the formation of large number of crystal nuclei occurs. Later, the process of growth of the particles is developed by diffusion. In our synthesis, the final solution does not present the supersaturation, although the nucleation process could occur when the zinc nitrate solution was added to the cobalt and dodecylamine solution, and the process of growth carried out is during the stirring of the final colloidal solution [31, 40]. On the other hand, the dodecylamine plays a key role in the microstructure of $ZnCo_2O_4$ particles, since the dodecylamine in the colloidal solution affects the particle growth via the saturating of nanocrystal surfaces and hence, results in the formation of $ZnCo_2O_4$ nanoparticles with a peculiar morphology (faceted nanoparticles were obtained) [28]. With thermal treatment at 500°C, the dodecylamine was finally removed from the $ZnCo_2O_4$ sample.

Figure 4 shows the typical TEM images of the $ZnCo_2O_4$ powder calcined at 500°C. **Figure 4a** exhibits a high concentration of nanoparticles, which was also observed by SEM. As can be seen **Figure 4b**, faceted nanoparticles with a pockmarked structure were clearly identified. The average particle size was ~75 nm, with a standard deviation of ±12.6 nm. A typical HRTEM image is displayed in **Figure 4c**. This image confirmed the presence of faceted nanoparticles and a value of 0.286 nm corresponded to the inter-planar d-spacing of the (200) plane of $ZnCo_2O_4$ spinel structure.

In order to investigate the nanoparticle's composition, EDS line scan was performed on $ZnCo_2O_4$ powder. **Figure 5** shows the corresponding analysis. **Figure 5a** shows a HAADF-STEM image of the $ZnCo_2O_4$ nanoparticles. The image confirms the presence of faceted nanoparticles with a pockmarked structure, which is consistent with the TEM images. In the EDS line scan, zinc, cobalt, and oxygen are observed across the linear mapping, confirming the presence of the expected elements, as seen in **Figure 5b**. In the central region X_2, a

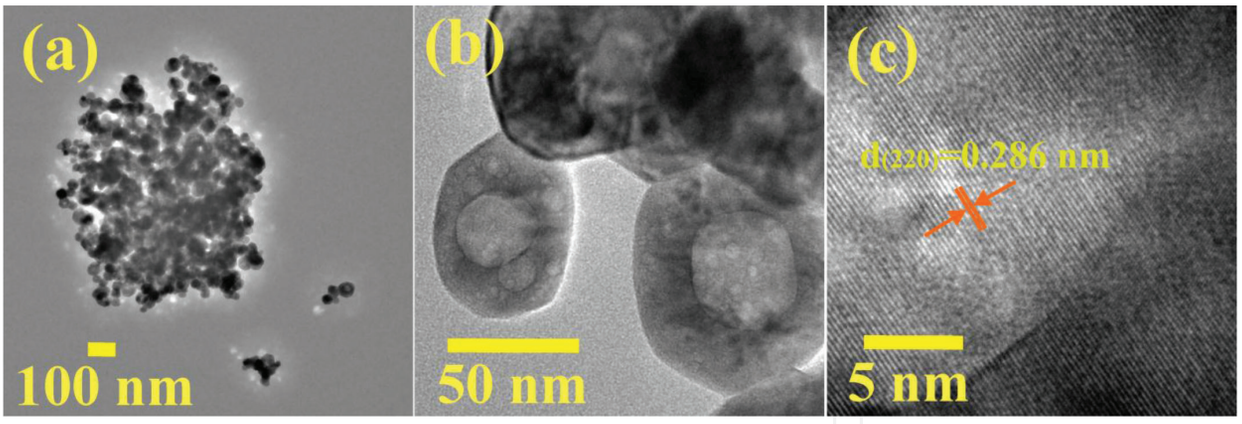

Figure 4. (a, b) TEM and (c) HRTEM images of $ZnCo_2O_4$.

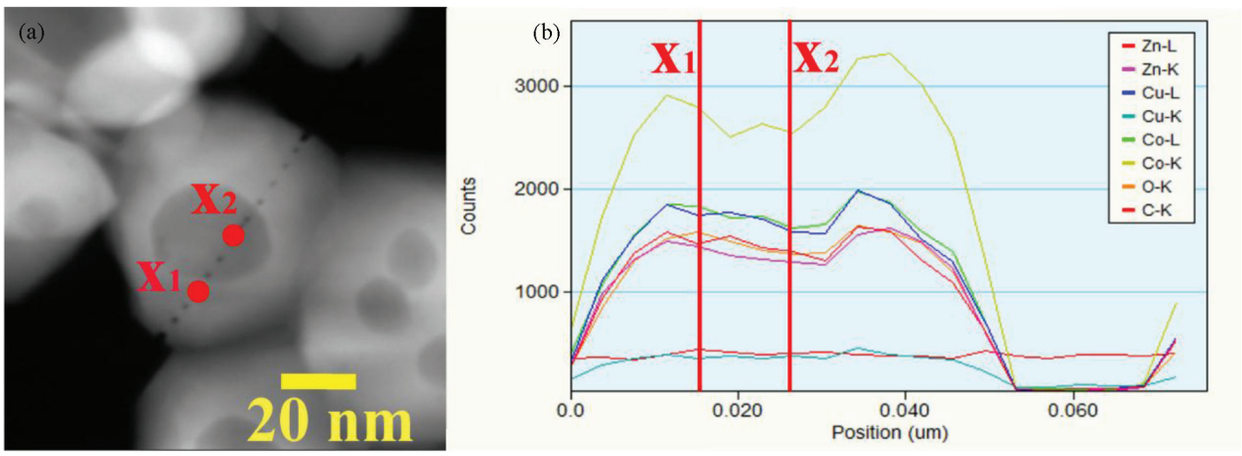

Figure 5. (a) HAADF-STEM image and (b) EDS elemental line scan of an individual $ZnCo_2O_4$ nanoparticle.

decrease of the element composition is observed in comparison to point X_1, which can be due to the irregular surface of the nanoparticle (pockmarked zone). It is also evident that cobalt exists in larger amount than zinc, corresponding to the target ratio of 1:2. However, the EDS line scan shows carbon (C) and copper (Cu) compounds, which are due to the sample support.

2.5. Raman characterization

The Raman spectrum shown in **Figure 6** allowed us to confirm the formation of the $ZnCo_2O_4$ when a calcination temperature of 500°C was used. As shown in **Figure 6**, the Raman spectrum of the $ZnCo_2O_4$ powder shows five vibrational bands located at 182, 475, 516, 613, and 693 cm^{-1} corresponding to the five active Raman bands of $ZnCo_2O_4$ spinel structure [41]. However, the band at 204 cm^{-1} is a vibrational mode that could be generated by Co_3O_4 [42]. The formation of this oxide is due to the cation disorder (substitution of Zn^{2+} by Co^{2+}) in

http://dx.doi.org/10.5772/68043

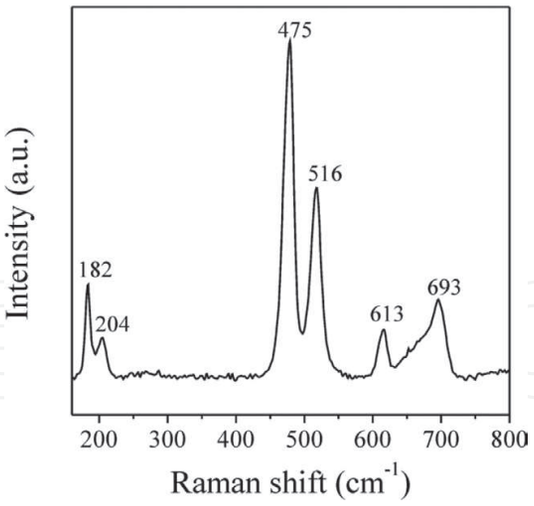

Figure 6. Raman spectrum of nanostructured $ZnCo_2O_4$ powder [37].

the $ZnCo_2O_4$ spinel structure. As the Co_3O_4 possess a spinel structure same as the $ZnCo_2O_4$; therefore, they have similar XRD patterns and a deformation in the XRD pattern of $ZnCo_2O_4$ is not expected.

2.6. Gas sensing application of $ZnCo_2O_4$

The sensing performance of the $ZnCo_2O_4$ sensor was investigated on pellets fabricated from the nanostructured $ZnCo_2O_4$ powders and tested in different concentrations of CO. **Figure 7** shows the variation of sensitivity against temperature at different concentrations of CO (1, 5, 50, 100, 200, and 300 ppm). As shown in **Figure 7**, only minor variations in sensitivity were measured at operating temperatures between 100 and 200°C in whole CO concentration range (1–300 ppm). For operating temperatures above 200°C, the sensitivity increased markedly from 5 to 300 ppm, with the maximum values of the sensitivity registered at 300°C.

Figure 8 shows sensitivity of the $ZnCo_2O_4$ sensor toward different concentrations of CO at 100, 200, and 300°C. As seen in **Figure 8a**, a sensitivity value of 1 was maintained across the CO concentration range when the $ZnCo_2O_4$ sensor was operated at 100°C. On the contrary, when the $ZnCo_2O_4$ sensor was working at a temperature of 200°C (**Figure 8a**) and 300°C (**Figure 8b**), the sensitivity increased with an increase of CO concentration. At 200°C, the sensitivity values of the sensor were 1, 1.1, 1.5, 2.2, 2.8, and 3.1 for CO concentrations of 1, 5, 50, 100, 200, and 300 ppm, respectively. However, at 300°C and with same concentrations, the sensitivity values were 1, 2, 3.3, 84.5, 157.5, and 305, respectively. The observed increase in sensitivity with the concentration is due to increase in gas concentration and operation temperature. The increase of the sensitivity is also associated with increased oxygen desorption at high temperatures [43, 44]. Additionally, the $ZnCo_2O_4$ sensor showed a decrease in gas response when CO gas were removed from the vacuum chamber.

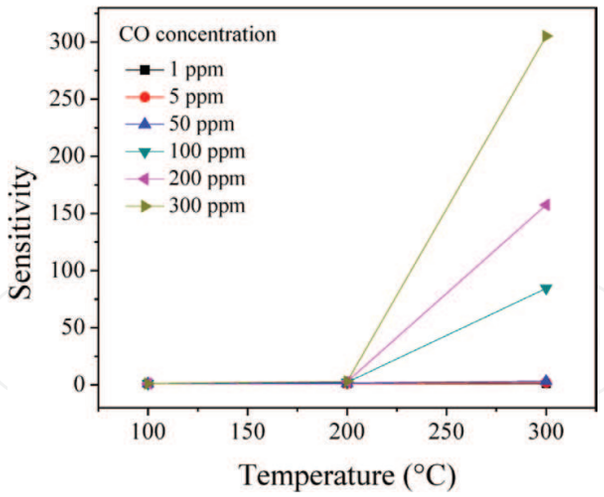

Figure 7. Sensitivity of the $ZnCo_2O_4$ sensor as a function of the temperature.

It is known that the gas sensing mechanism of semiconducting materials is based on the changes of the electrical resistance produced by interaction between the target gas and chemisorbed oxygen ions [45, 46]. When oxygen is adsorbed on the semiconductor's surface, oxygen species are generated at the surface by taking electrons from the conduction band of the semiconductor. In general, molecular (O_2^-) and ionic (O^- and O^{2-}) species are formed below 150°C and above this temperature, respectively [47]. Consequently, a space charge layer with thickness of ~100 nm is formed at the surface [6]. In our tests at temperatures above 100°C, the ionic species that adsorb chemically on the sensor are more reactive than molecular species that adsorb at temperatures below 100°C [30, 33, 48]. It means that below 100°C, the thermal energy is not enough to produce the desorption reactions of the oxygen and, therefore, an

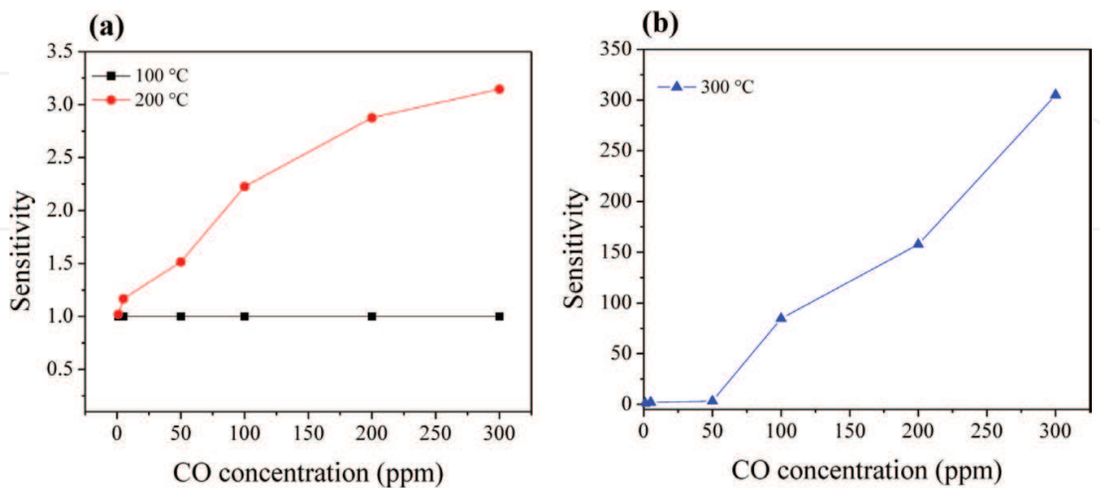

Figure 8. Sensitivity of the $ZnCo_2O_4$ sensor vs. concentration at different temperatures: (a) 100 and 200°C and (b) 300°C.

electrical response does not occur regardless of the gas concentration, as can see in **Figure 8a**. By contrast, above 100°C (in this case 200 and 300°C), the formation of ionic species at surface of the $ZnCo_2O_4$ occurs causing a chemical reaction with the gas and resulting in changes in the electrical resistance of the material (i.e., a high sensitivity is recorded) [48, 49]. Additionally, the conductivity mechanism of $ZnCo_2O_4$ sensor is strongly related to the crystallite size (D) and the space charge layer (L): if $D >> 2L$, the conductivity is limited by the Schottky barrier at the particle border; thus, gas detection does not depend on the size of the particle; if $D = 2L$, the conductivity and the gas sensing depend on the growing of necks formed by crystallites; and when $D < 2L$, the conductivity depends on the size of the crystallites [2]. In our case, the latter condition occurs while detecting the gases, since the average particle size is less than 100 nm; that is the reason why the conduction of the charge carriers (holes) takes place on the nanoparticles' surface [6, 50].

In comparison with previous works, our $ZnCo_2O_4$ sensor fabricated on faceted nanoparticles showed a superior sensitivity toward CO (a sensitivity of ~305 in 300 ppm of CO at 300°C) than those sensors based on $ZnCo_2O_4$ nanoparticles [18], hierarchical porous $ZnCo_2O_4$ nano/microspheres [19], $ZnCo_2O_4$ nanotubes [20], porous $ZnO/ZnCo_2O_4$ hollow spheres [21], and nanowires-assembled hierarchical $ZnCo_2O_4$ microstructure [25], with sensitivities of 1 (50 ppm at 350°C), 2 (100 ppm at 175°C), 1.69 (400 ppm at 300°C), 1.1 (100 ppm at 275°C), and 29 (10 ppm at 300°C), respectively.

2.7. Conclusions

$ZnCo_2O_4$-faceted nanoparticles (~75 nm) were obtained by the simple and inexpensive microwave-assisted colloidal method, using dodecylamine as surfactant. This synthetic method is allowed to obtain the $ZnCo_2O_4$ at a calcination temperature of 500°C. The sensing tests showed that $ZnCo_2O_4$ sensor is highly sensitive to concentrations of 1–300 ppm of carbon monoxide at working temperatures above 100°C. Specifically, a maximum sensitivity of 305 was obtained for a CO concentration of 300 ppm at a working temperature of 300°C. The CO sensing response of $ZnCo_2O_4$ is better than that reported in previous investigations. Therefore, $ZnCo_2O_4$ can be considered as a potential candidate for gas sensing applications.

Acknowledgements

The authors are grateful to PRODEP for financial support under the project F-PROMEP-39/Rev-04 SEP-23-005. The authors also thank PROFOCIE 2016 for financial support and CONACYT-México grants: the National Laboratory for Nanoscience and Nanotechnology Research (LINAN). The authors are grateful to G. J. Labrada-Delgado, B. A. Rivera-Escoto, K. Gomez, Miguel Ángel Luna-Arias and Sergio Oliva for their technical assistance.

Author details

Juan Pablo Morán-Lázaro[1]*, Florentino López-Urías[2], Emilio Muñoz-Sandoval[2], Oscar Blanco-Alonso[3], Marciano Sanchez-Tizapa[4], Alejandra Carreon-Alvarez[4], Héctor Guillén-Bonilla[5], María de la Luz Olvera-Amador[6], Alex Guillén-Bonilla[1] and Verónica María Rodríguez-Betancourtt[7]

*Address all correspondence to: lazaro7mx27@gmail.com

1 Department of Computer Science and Engineering, CUValles, University of Guadalajara, Ameca, Jalisco, Mexico

2 Advanced Materials Department, IPICYT, San Luis Potosí, S.L.P., Mexico

3 Department of Physics, CUCEI, University of Guadalajara, Guadalajara, Jalisco, Mexico

4 Department of Natural and Exact Sciences, CUValles, University of Guadalajara, Ameca, Jalisco, Mexico

5 Department of Project Engineering, CUCEI, University of Guadalajara, Guadalajara, Jalisco, Mexico

6 Department of Electrical Engineering (SEES), CINVESTAV-IPN, Mexico City, DF, Mexico

7 Department of chemistry, CUCEI, University of Guadalajara, Guadalajara, Jalisco, Mexico

References

[1] Yamazoe N, Shimanoe K. New perspectives of gas sensor technology. Sens. Actuators B. 2009;**138**:100-107. DOI: 10.1016/j.snb.2009.01.023

[2] Xu C, Tamaki J, Miura N, Yamazoe N. Grain size effects on gas sensitivity of porous SnO_2-based elements. Sens. Actuators B. 1991;**3**:147-155. DOI: 10.1016/0925-4005(91)80207-Z

[3] Du J, Zhao R, Xie Y, Li J. Size-controlled synthesis of SnO_2 quantum dots and their gas-sensing performance. App. Surf. Sci. 2015;**346**:256-262. DOI: 10.1016/j.apsusc.2015.04.011

[4] Wan Q, Li QH, Chen YJ, Wang TH, He XL, Li JP, Lin CL. Fabrication and ethanol sensing characteristics of ZnO nanowire gas sensors. App. Phys. Lett. 2004;**84**:3654-3656. DOI: 10.1063/1.1738932

[5] Lin S, Wu J, Akbar SA. A selective room temperature formaldehyde gas sensor using TiO_2 nanotube arrays. Sens. Actuators B. 2011;**156**:505-509. DOI: 10.1016/j.snb.2011.02.046

[6] Kim HJ, Lee JH. Highly sensitive and selective gas sensors using p-type oxide semiconductors: overview. Sens. Actuators B. 2014;**192**:607-627. DOI: 10.1016/j.snb.2013.11.005

[7] Sharma Y, Sharma N, Subba-Rao GV, Chowdari BVR. Nanophase $ZnCo_2O_4$ as a high performance anode material for Li-ion batteries. Adv. Funct. Mater. 2007;**17**:2855-2861. DOI: 10.1002/adfm.200600997

[8] Du N, Xu Y, Zhang H, Yu J, Zhai C, Yang D. Porous $ZnCo_2O_4$ nanowires synthesis via sacrificial templates: high-performance anode materials of Li-ion batteries. Inorg. Chem. 2011;**50**:3320-3324. DOI: 10.1021/ic102129w

[9] Huang L, Waller GH, Ding Y, Chen D, Ding D, Xi P, Wang ZL, Liu M. Controllable interior structure of $ZnCo_2O_4$ microspheres for high-performance lithium-ion batteries. Nano Energy 2015;**11**:64-70. DOI: 10.1016/j.nanoen.2014.09.027

[10] Bai J, Li X, Liu G, Qian Y, Xiong S. Unusual formation of $ZnCo_2O_4$ 3D hierarchical twin microspheres as a high-rate and ultralong-life lithium-ion battery anode material. Adv. Funct. Mater. 2014;**24**:3012-3020. DOI: 10.1002/adfm.201303442

[11] Liu B, Zhang J, Wang X, Chen G, Chen D, Zhou C, Shen G, Qian Y, Xiong S. Hierarchical three-dimensional $ZnCo_2O_4$ nanowire arrays/carbon cloth anodes for a novel class of high-performance flexible lithium-ion batteries. Nano Lett. 2012;**12**:3005-3011. DOI: 10.1021/n1300794f

[12] Zhou G, Zhu J, Chen Y, Mei L, Duan X, Zhang G, Chen L, Wang T, Lu B. Simple method for the preparation of highly porous $ZnCo_2O_4$ nanotubes with enhanced electrochemical property for supercapacitor. Electrochim. Acta. 2014;**123**:450-455. DOI: 10.1016/j.electacta.2014.01.018

[13] Wu C, Cai J, Zhang Q, Zhou X, Zhu Y, Li L, Shen P, Zhang K. Direct growth of urchin-like $ZnCo_2O_4$ microspheres assembled from nanowires on nickel foam as high-performance electrodes for supercapacitors. Electrochim. Acta. 2015;**169**:202-209. DOI: 10.1016/j.electacta.2015.04.079

[14] Fu W, Li X, Zhao C, Liu Y, Zhang P, Zhou J, Pan X, Xie E. Facile hydrothermal synthesis of flower like $ZnCo_2O_4$ microspheres as binder-free electrodes for supercapacitors. Mater. Lett. 2015;**169**:202-209. DOI: j.matlet.2015.02.092

[15] Chang SK, Zainal Z, Tan KB, Yusof NA, Yusoff WMDW, Prabaharan SRS. Recent development in spinel cobaltites for supercapacitor application. Ceram. Int. 2015;**41**:1-14. DOI: 10.1016/j.ceramint.2014.07.101

[16] Gawande KB, Gawande SB, Thakare SR, Mate VR, Kadam SR, Kale BB, Kulkarni MV. Effect of zinc: cobalt composition in $ZnCo_2O_4$ spinels for highly selective liquefied petroleum gas sensing at low and high temperatures. RSC Adv. 2015;**5**:40429-40436. DOI: 10.1039/c5ra03960f

[17] Mariappan CR, Kumara R, Vijaya P. Functional properties of $ZnCo_2O_4$ nano-particles obtained by thermal decomposition of a solution of binary metal nitrates. RSC Adv. 2015;**5**:26843-26849. DOI: 10.1039/c5ra01937k

[18] Vijayanand S, Joy PA, Potdar HS, Patil D, Patil P. Nanostructured spinel $ZnCo_2O_4$ for the detection of LPG. Sens. Actuators B. 2011;**152**:121-129. DOI: 10.1016/j.snb.2010.09.001

[19] Liu T, Liu J, Liu Q, Song D, Zhang H, Zhang H, Wang J. Synthesis, characterization and enhanced gas sensing performance of porous $ZnCo_2O_4$ nano/microspheres. Nanoscale. 2015;**7**:19714-19721. DOI: 10.1039/c5nr05761b

[20] Zhang, GY, Guo B, Chen J. MCo_2O_4 (M = Ni, Cu, Zn) nanotubes: template synthesis and application in gas sensors. Sens. Actuators B. 2006;**114**:402-409. DOI: j.matlet. 2015.02.092

[21] Zhou X, Feng W, Wang C, Hu X, Li X, Sun P, Shimanoe K, Yamazoe N, Lu G. Porous $ZnO/ZnCo_2O_4$ hollow spheres: synthesis, characterization, and applications in gas sensing. J. Mater. Chem. A. 2014;**2**:17683-17690. DOI: 10.1039/c4ta04386c

[22] Niu X, Du W, Du W. Preparation and gas sensing properties of ZnM_2O_4 (M = Fe, Co, Cr). Sens. Actuators B. 2004;**99**:405-409. DOI: 10.1016/j.snb.2003.12.007

[23] Park HJ, Kim J, Choi NJ, Song H, Lee DS. Nonstoichiometric Co-rich $ZnCo_2O_4$ hollow nanospheres for high performance formaldehyde detection at ppb levels. ACS Appl. Mater. Interfaces. 2016;**8**:3233-3240. DOI: 10.1021/acsami.5b10862

[24] Qu F, Jiang H, Yang M. Designed formation through a metal organic framework route of $ZnO/ZnCo_2O_4$ hollow core–shell nanocages with enhanced gas sensing properties. Nanoscale. 2016;**8**:16349-16356. DOI: 10.1039/c6nr05187a

[25] Long H, Harley-Trochimczyk A, Cheng S, Hu H, Chi WS, Rao A, Carraro C, Shi T, Tang Z, Maboudian R. Nanowire-assembled hierarchical $ZnCo_2O_4$ microstructure integrated with a low-power microheater for highly sensitive formaldehyde detection. ACS Appl. Mater. Interfaces. 2016;**8**:31764-31771. DOI: 10.1021/acsami.6b11054

[26] Wei X, Chen D, Tang W. Preparation and characterization of the spinel oxide $ZnCo_2O_4$ obtained by sol–gel method. Mater. Chem. Phys. 2007;**103**:54-58. DOI: 10.1016/j.matchemphys.2007. 01.006

[27] Wang Y, Wang M, Chen G, Dong C, Wang Y, Fan LZ. Surfactant-mediated synthesis of $ZnCo_2O_4$ powders as a high-performance anode material for Li-ion batteries. Ionics. 2015;**21**:623-628. DOI: 10.1007/s11581-014-1221-1

[28] Morán-Lázaro JP, Blanco O, Rodríguez-Betancourtt VM, Reyes-Gómez J, Michel CR. Enhanced CO_2-sensing response of nanostructured cobalt aluminate synthesized using a microwave-assisted colloidal method. Sens. Actuators B. 2016;**226**:518-524. DOI: 10.1016/j. snb.2015.12.013

[29] Guillen-Bonilla H, Reyes-Gomez J, Guillen-Bonilla A, Pozas-Zepeda D, Guillen-Bonilla JT, Gildo-Ortiz L, Flores-Martinez M. Synthesis and characterization of $MgSb_2O_6$ trirutile-type in low presence concentrations of ethylenediamine. J. Chem. Chem. Eng. 2013;**7**: 395-401.

[30] Guillén-Bonilla A, Rodríguez-Betancourtt VM, Flores-Martínez M, Blanco-Alonso O, Reyes-Gómez J, Gildo-Ortiz L, Guillén-Bonilla H. Dynamic response of $CoSb_2O_6$ trirutile-type oxides in a CO_2 atmosphere at low-temperatures. Sensors. 2014;**14**:15802-15814. DOI: 10.3390/s140915802

[31] Blanco O, Morán-Lázaro JP, Rodríguez-Betancourtt VM, Reyes-Gómez J, Barrera A. Colloidal synthesis of $CoAl_2O_4$ nanoparticles using dodecylamine and their structural characterization. Superficies y Vacío. 2016;**29**:78-82.

[32] Guillen-Bonilla H, Rodríguez-Betancourtt VM, Guillén-Bonilla JT, Reyes-Gómez J, Gildo-Ortiz L, Flores-Martínez M, Olvera-Amador ML, Santoyo-Salazar J. CO and C_3H_8 sensitivity behavior of zinc antimonate prepared by a microwave-assisted solution method. J. Nanomater. 2015;**2015**:1-8. DOI: 10.1155/2015/979543

[33] Guillén-Bonilla H, Flores-Martínez M, Rodríguez-Betancourtt VM, Guillén-Bonilla A, Reyes-Gómez J, Gildo-Ortiz L, Olvera-Amador ML, Santoyo-Salazar J. A novel gas sensor based on $MgSb_2O_6$ nanorods to indicate variations in carbon monoxide and propane concentrations. Sensors. 2016;**16**:177-188. DOI: 0.3390/s16020177

[34] Guillén-Bonilla H, Gildo-Ortiz L, Olvera ML, Santoyo-Salazar J, Rodríguez-Betancourtt VM, Guillen-Bonilla A, Reyes-Gómez J. Sensitivity of mesoporous $CoSb_2O_6$ nanoparticles to gaseous CO and C_3H_8 at low temperatures. J. Nanomater. 2015;**2015**:1-9. DOI: 10.1155/2015/308465

[35] Mirzaei A, Neri G. Microwave-assisted synthesis of metal oxide nanostructures for gas sensing application: a review. Sens. Actuators B. 2016;**237**:749-775. DOI: 10.1016/j.snb.2016.06.114

[36] Hu SY, Lee YC, Chen BJ. Characterization of calcined $CuInS_2$ nanocrystals prepared by microwave-assisted synthesis. J. Alloys Compd. 2017;**690**:15-20. DOI: 10.1016/j.jallcom.2016.08.098

[37] Morán-Lázaro JP, López-Urías F, Muñoz-Sandoval E, Blanco-Alonso O, Sanchez-Tizapa M, Carreon-Alvarez A, Guillén-Bonilla H, Olvera-Amador ML, Guillén-Bonilla A, Rodríguez-Betancourtt. Synthesis, characterization, and sensor applications of spinel $ZnCo_2O_4$ nanoparticles. Sensors. 2016;**16**:2162. DOI: 10.3390/s16122162

[38] Ji Y, Zhao Z, Duan A, Jiang G, Liu J. Comparative study on the formation and reduction of bulk and Al_2O_3-supported cobalt oxides by H_2-TPR technique. J. Phys. Chem. C. 2009;**113**:7186-7199. DOI: 10.1021/jp8107057

[39] LaMer VK, Dinegar RH. Theory, production and mechanism of formation of monodispersed hydrosols. J. Am. Chem. Soc. 1950;**72**:4847-4854. DOI: 10.1021/ja01167a001

[40] Vekilov PG. What determines the rate of growth of crystals from solution? Cryst Growth Des. 2007;**7**:2796-2810. DOI: 10.1021/cg070427i

[41] Samanta K, Bhattacharya P, Katiyar RS. Raman scattering studies in dilute magnetic semiconductor $Zn_{1-x}Co_xO$. Phys. Rev. B. 2006;**73**:245213-245215. DOI: 10.1103/PhysRevB.73.245213

[42] Shirai H, Morioka Y, Nakagawa I. Infrared and Raman spectra and lattice vibrations of some oxide spinels. J. Phys. Soc. Jpn. 1982;**51**:592-597. DOI: 10.1143/JPSJ.51.592

[43] Chang SC. Oxygen chemisorption on tin oxide: correlation between electrical conductivity and EPR measurements. J. Vac. Sci. Technol. 1979;**17**:366-369. DOI: 10.1116/1.570389

[44] Gildo-Ortiz L, Guillén-Bonilla H, Santoyo-Salazar J, Olvera ML, Karthik TVK, Campos-González E, Reyes-Gómez J. Low-temperature synthesis and gas sensitivity of perovskite-type $LaCoO_3$ nanoparticles. J. Nanomater. 2014;**2014**:1-8. DOI: 10.1155/2014/164380

[45] Yamazoe N. New approaches for improving semiconductor gas sensors. Sens. Actuators B. 1991;**5**:7-19. DOI: 10.1016/0925-4005(91)80213-4

[46] Moseley PT. Materials selection for semiconductor gas sensors. Sens. Actuators B. 1992;**6**:149-156. DOI: 10.1016/0925-4005(92)80047-2

[47] Bochenkov VE, Sergeev GB. Preparation and chemiresistive properties of nanostructured materials. Adv. Colloid Interface Sci. 2005;**116**:245-254. DOI: 10.1016/j.cis.2005.05.004

[48] Wang C, Yin L, Zhang L, Xiang D, Gao R. Metal oxide gas sensors: sensitivity and influencing factors. Sensors. 2010;**10**:2088-2106. DOI: 10.3390/s100302088

[49] Yamazoe, N. Toward innovations of gas sensor technology. Sens. Actuators B. 2005;**108**:2-14. DOI: 10.1016/j.snb.2004.12.075

[50] Tan OK, Cao W, Hu Y, Zhu W. Nano-structured oxide semiconductor materials for gas-sensing applications. Ceram. Int. 2004;**30**:1127-1133. DOI: 10.1016/j.ceramint.2003.12.015